



Shear alters wax appearance in mineral oil + paraffin wax mixtures

Sedi Helsper¹ · Abdualbaset A. Ali¹ · Matthew W. Liberatore¹

Received: 18 February 2021 / Revised: 29 April 2021 / Accepted: 13 June 2021 / Published online: 14 July 2021
© The Author(s), under exclusive licence to Springer-Verlag GmbH Germany, part of Springer Nature 2021

Abstract

Wax deposition is a challenge in crude oil transportation. Wax deposition is affected by many factors, including cooling rate and wax concentration. However, the effect of shear rate on wax appearance temperature (WAT) is less studied, so an investigation of a model waxy oil system, mineral oil and paraffin wax, was undertaken. Wax appearance temperature was depressed by different extents by increasing shear rate, increasing cooling rate, and decreasing wax concentration. Corroborating other studies, wax concentration significantly affected WAT. Changing concentration from 5 to 50 wt% resulted in ~20 °C increase in WAT. Two types of rheological measurements were completed for determining WAT under shear, either a temperature ramp or isothermal steps. Both techniques found WAT within 1 °C of the other. Overall, shear rate has a small, quantifiable effect on WAT of ~2 °C when changing from 1 to 1000 s⁻¹ at the same cooling rate. Similarly, a decrease in cooling rate from 10 to 0.2 °C/min under 100 s⁻¹ shear increased WAT ~4 °C. In addition, yield stress decreased from 416 to 8 Pa with increasing shear upon wax formation from 0 to 1000 s⁻¹. Increasing cooling rate from 0.2 to 5 °C/min increased yield stress from 5 to 505 Pa when formed at 10 s⁻¹. Wax appearance studies using rheology were corroborated by static techniques, including calorimetry and phase behavior. Overall, adding shear rate to the phase diagrams of waxy oils could help the industry address their flow assurance needs.

Keywords Wax · Wax appearance temperature · Oil · Rheology · Yield stress · Flow assurance

Introduction

A significant problem with the transportation of crude oils is the deposition of waxes that lead to the blockage of pipelines (Flavio S. Ribeiro et al. 1997; Sun et al. 2019). The process of pipeline blockage occurs in three stages: precipitation, deposition, and complete gelation, which nominally require between 1 and 6 wt% wax (Chala et al. 2018). Wax deposition is the formation of solids that can grow on a surface, lead to damage near the wellbore, or cause changes in fluid properties as wax precipitates out of the liquid phase (Singh et al. 2000). The concentration of solute in excess of saturation, lateral transport by diffusion, shear dispersion, Brownian diffusion, and gravity settling provide driving forces for

the formation of wax particles (Lashkarbolooki et al. 2011; Zhu et al. 2008). In addition, wax clusters can trap oil and create large gel-like structures with high viscosity (Theyab 2018).

Wax precipitation and flow assurance issues are affected by many factors, including oil composition, flow rate, temperature gradient, pipe wall temperature, oil temperature, shear stress, recirculation time of oil in the rig, and oil viscosity (Lee 2008; Theyab and Yahya 2018). Temperature is probably the most critical factor in wax precipitation and deposition because of its effects on solubility, e.g., paraffin wax is liquid at reservoir temperatures of between 70 and 150 °C (Thota and Onyeanuna 2016). Wax solubility decreases with decreasing temperature, and the rate of deposition is proportional to the temperature difference between the bulk oil and pipe wall (Thota and Onyeanuna 2016; Zhu et al. 2008).

Since wax concentration differs by location, oil composition plays an important role in wax deposition (Coutinho and Daridon 2005; García 2000). The effect of wax content on wax appearance temperature is an important variable in many

Sedi Helsper and Abdualbaset A. Ali contributed equally to this work

✉ Matthew W. Liberatore
matthew.liberatore@utoledo.edu

¹ Department of Chemical Engineering, University of Toledo, Toledo, OH, USA

studies (e.g., Dimitriou and McKinley 2014; Dimitriou et al. 2011). While wax may cause problems in pipelines, wax is useful in other situations. Paraffin wax with about 3–7 wt% oil is used to make paper and food packages impermeable to water. Other, natural waxes at concentrations of 5–79 wt% are used in household chemicals such as shoe, floor, furniture, and automobile polishes, or candle manufacture (Freund et al. 1982). Some cosmetics, such as lipsticks, use 10–12 wt% wax to create consistent performance (Freund et al. 1982).

Various laboratory techniques have been developed to measure wax properties, such as differential scanning calorimetry (DSC), cross polar microscopy (CPM), and rheometry. DSC measures the heat given off during a crystallization or phase change process. An exothermic peak appears as wax precipitates, indicating the wax appearance temperature (WAT). DSC also measures the total heat flux of wax precipitation. Since this method measures heat, both transparent and opaque samples can be measured. Alternatively, enhanced contrast between liquid and solid improves the applicability of CPM for detecting the WAT in crude oils that can be dark in color and/or opaque (Yang et al. 2015).

WAT can also be determined with rheological methods by measuring viscosity as temperature decreases. WAT is recorded when the viscosity increases significantly (Tarantino, 2016). WAT under flow is also called gelation temperature (GT). In this paper, we follow the convention that WAT and GT are synonymous terms similar to other works (Alcazar-Vara and Buenrostro-Gonzalez 2011). Flow rate affects wax deposition because different forces dominate flow under different flow regimes (Theyab 2018). Under turbulent flow, dynamic forces maintain fluid flow parallel to the pipe axis and allow for mixing between layers. Contrarily, under laminar flow, viscous forces prevent mixing between layers. Laboratory studies indicate that under a laminar flow regime, wax deposition is more prevalent when compared to turbulent flow (Hsu and Brubaker 1995; Lee 2008).

Many publications have investigated the effect of cooling on WAT or wax strength under static conditions (Lin et al. 2011; Ruwoldt et al. 2018). Others have determined cooling effects on wax appearance using rheometry. However, many of these experiments have been done at relatively small shear rates that mimic static conditions (Japper-Jaafar et al. 2016b; Rønningsen 1992). Varying shear rate is important in order to investigate features of waxy crude oil, such as morphology of wax particles or thixotropy after precipitation (Hénaut et al. 1999; Kane et al. 2002). However, little work probed the effect of shear rate on wax appearance. In this paper, we will quantify how WAT changes over wide ranges of shear rate (1 to 1000 s⁻¹), concentration (5 to 50 wt%), and temperature gradient (0.2 to 10 °C/min).

Experimental

Materials

Mixing a commercial mineral oil and paraffin wax at different concentrations serves as an analog for a waxy crude oil. Paraffin wax is the predominant wax type in crude oils and can cause blockage in pipelines upon solidification (Kurniawan et al. 2018). Paraffin wax and light mineral oil (LMO) were sourced from Sigma Aldrich. LMO has a density at 25 °C of 0.838 g/L and a flash point of 112 °C, while paraffin wax flashes at 113 °C and melts between 58 and 62 °C.

Waxy oil samples were prepared at six different mass concentrations: 5, 10, 15, 25, 35, and 50 wt% wax in LMO. An amount of solid wax was measured and mixed with LMO. After heating the sample using hot plate (> 80 °C), a single-phase liquid was created and further studied. Samples were stored in a water bath at 80 °C to ensure that samples remained a single-phase liquid.

Methods

The wax appearance temperature of various compositions of paraffin wax in LMO was observed at static conditions using two methods. First, samples were placed in a temperature-controlled water bath, which used ASTM D2500 to determine WAT (Hammami et al. 2003). Secondly, differential scanning calorimeter (DSC) confirmed WAT thermally (Zhao et al. 2015).

More specifically, samples at various wax concentrations were placed in a temperature-controlled water bath. Phase observations began at 65 °C, which is above melting point of pure wax (58–62 °C). Temperature was lowered by 1 °C from 65 to 10 °C with at least 1 h equilibration time per temperature step. Visual inspection determined cloud point, viscous appearance, pour point, and solid phase. Cloud point represents the temperature where wax particles first start to agglomerate, demonstrating some opacity compared to the previously transparent liquid. Pour point describes the temperature at which a sample ceases to flow freely when tilting a vial for at least 5 s. After the pour point is observed, a final phase change may be observed upon further cooling when the sample becomes a white solid.

Waxy oil samples, stored at 80 °C, were weighed (~7 mg) in a stainless-steel pan to perform DSC (DSC 250 from TA Instruments) using standard protocols. Each sample was equilibrated at 65 °C for 5 min, analogous to the phase study and rheological experiments. To determine the WAT, temperature ranged from 65 to 15 °C at a

cooling rate of 10 °C/min. WAT was determined by onset temperature. The onset temperature is represented by the section of the heat flow curve where the heat flow begins to increase significantly. The onset temperature was calculated by finding the tangent point where the slope changes between the horizontally and vertically directed lines on the graph (Hansen et al. 1991; Zhao et al. 2015). The onset temperature was recorded as the WAT.

Flow measurements were carried out using a Discovery Hybrid Rheometer (DHR3) from TA Instruments. All experiments, except yield stress measurements, used a 60-mm stainless-steel parallel plate geometry at a gap of 500 μm in conjunction with a temperature-controlled Peltier plate (± 0.1 °C). Before beginning rheological experiments, all samples were conditioned for 1 min to erase the thermal history by pre-shearing at 65 °C and 1 s^{-1} .

Viscosity was measured by two methods. Temperature ramp experiments cooled samples from 65 to 5 °C below the wax appearance temperature determined in water bath experiments. Experiments were run at temperature ramp rates of 10, 5, 2, 1, 0.5, and 0.2 °C/min. Moreover, flow measurements were taken at constant temperature 5 °C below WAT for each sample. Steady state measurements at shear rates varied from 1 to 1000 s^{-1} . Every experiment was run three times, and standard deviations were calculated.

One method for determining WAT or gelation temperature is when viscosity deviates from an Arrhenius model fit (Alcazar-Vara and Buenrostro-Gonzalez 2011). Since the temperature dependence of Newtonian fluids fits an Arrhenius equation well, WAT can be identified when viscosities diverge from the Arrhenius scaling (Li et al. 2015; Vargas et al. 2018). Alternatively, the ratio between viscosity at each time point to the time point before was calculated. A significant increase in this viscosity ratio was observed when wax solidified. A viscosity ratio of 5 was used to identify WAT under flow. Data analysis using the two mentioned procedures showed very good agreement (0.4–1.5% error) (see supporting information). Viscosity ratios are more easily calculated than Arrhenius fitting, so viscosity ratios are used throughout this paper.

In order to further investigate the effect of shear rate on WAT and eliminate temperature gradients, peak hold procedures were done at the same shear rates of temperature ramp experiments. Peak hold experiments were run at ± 3 °C from the WAT obtained from temperature ramp experiments. Each peak hold step measured viscosity for 120 s at a constant shear rate at 0.5 °C intervals. Thus, viscosity increases at both constant temperature and shear rate provides another measure of WAT.

To better investigate on the effect of shear rate and cooling rate on mechanical properties of the waxy solids, yield experiments were performed using a 28-mm vane and cup geometry. Initially, samples were cooled from 65 to

35 °C (~ 6 °C below pour point of 25 wt% wax/LMO sample) and held for 1 h. Oscillatory amplitude sweeps were done by increasing stress amplitude from 0.01 to 1000 Pa with frequency of 0.1 Hz. Experiments were terminated when oscillation strain $> 100\%$. Each amplitude sweep test took ~ 90 min. The maximum elastic stress ($= G'\gamma$) was defined as yield stress (Hagen 1993; Stickel 2009).

Results and discussion

Describing rheological features of pure components will occur first and frame the discussions of wax appearance temperature in LMO/wax mixtures. Then, effects of shear rate and cooling rate on 25 wt% wax (a representative sample) will be presented in detail. Concluding the “Results” section, measurements at other wax concentrations as well as under static conditions allow for comparisons with measurements under shear.

Pure components rheology

Understanding the rheology of each pure component provides content to discuss waxy oil mixtures. Steady-state flow curves were measured for pure wax and LMO (Fig. 1). LMO viscosity was Newtonian across all temperatures (-5 to 65 °C). For example, viscosity of LMO at 20 °C was 0.03 ± 0.001 Pa·s, which is more than ten times the viscosity of water at the same temperature (0.001 Pa·s). Also, viscosity of light oil at 65 °C was constant (0.006 ± 0.0007 Pa·s).

For pure wax at 65 °C, Newtonian behavior was observed. However, lowering the temperature to ~ 10 °C below the

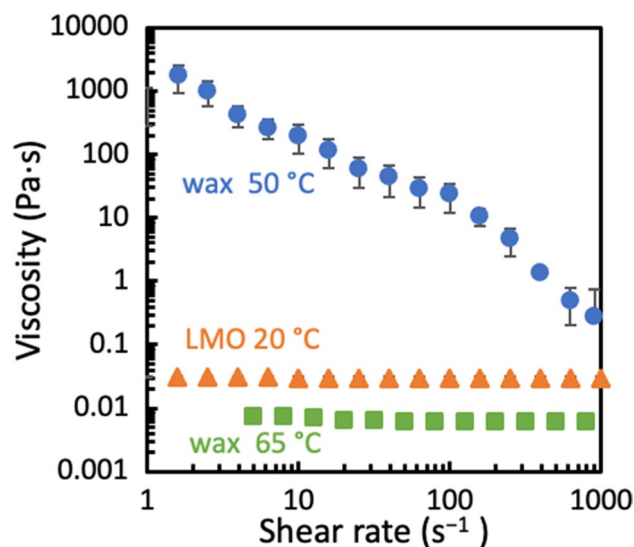


Fig. 1 Viscosity of pure LMO at 20 °C and pure paraffin wax at 50 °C and 65 °C

wax's melting point (50 °C), shear thinning was observed. By lowering the temperature from 65 to 50 °C, viscosity increased from 2 to 5 orders of magnitudes compared to the 65 °C wax between shear rates of 1 and 1000 s⁻¹. Viscosity of pure wax at 50 °C and shear rate 1 s⁻¹ is ~700 Pa·s, which is in the same order of magnitude as approximate viscosity of molten polymers (1000 Pa·s) (Hamada 2010). Overall, the rheology of pure oil and wax should bound the behavior of LMO with various concentrations of paraffin wax in subsequent sections.

Shear effects on WAT for 25 wt% wax

Detailed rheology on 25% wax provides quantitative detail on wax appearance under flow. At other wax concentrations, the rheology is qualitatively similar, so analyzed, aggregated results will be presented later. First, viscosity of 25 wt% wax at 65 °C and 5 °C above WAT showed Newtonian behavior up to 1000 s⁻¹ (Fig. 2). However, at 5 °C below the WAT, significant shear thinning was observed.

Since the model waxy oils are a two-component mixture of LMO and paraffin wax, rheological behavior can be compared with the pure components' properties. Wax solidification caused mixtures to increase significantly in viscosity below 100 s⁻¹ and demonstrate shear thinning once below the WAT. The increase in viscosity and shear thinning was measured at all wax concentrations at 5 °C below the WAT. After solid wax droplets form below the WAT, shear thinning can result from droplet deformation, i.e., wax droplets create more elliptical shapes that result in less collisions between droplets, and thus, decreasing viscosity (Mezger

2011). Alternatively, long chains of paraffin wax can reorient to structures that align with the flow under increasing shear rates (Visintin 2005; Wagner and Brady 2009). Another physical explanation of shear thinning is breaking of inter-particle bonds (e.g., van der Waals forces) between wax molecules formed during cooling (I.M.El-Gamal 1998; Winterton 1970). Shear thinning at 5 °C below the WAT can be represented by a power law, which will be elaborated on later.

For 25% wax in LMO, using the temperature ramp procedure, WAT at shear rates of 1, 10, 100, and 1000 s⁻¹ was measured at ambient pressure and cooling rate 0.2 °C/min to be 45.5 ± 0.1, 44.6 ± 0.5, 43.9 ± 0.1, and 43.2 ± 0.5 °C, respectively (Fig. 3). Therefore, increasing shear rate from 1 to 1000 s⁻¹ lowered the WAT more than 2 °C. Lower shear rates may allow wax clusters to form more readily (Japper-Jaafar et al. 2016b). One explanation is that shear minimizes time for wax nuclei to come in contact and form bigger clusters (Macosko 1994; Wessel and Ball 1992). Viscosity after the phase change at low shear rates (1 and 10 s⁻¹) increases by at least 100-fold by 2 or 3 °C below the WAT. However, applying higher shear rates, the increase in viscosity below the WAT is observed to be about threefold for shear rates 100 and 1000 s⁻¹.

For 25 wt% wax, yield stresses of waxy solids formed at shear rates of 0, 10, 100, and 1000 s⁻¹ were measured to be 416 ± 32, 145 ± 3, 46 ± 1, and 8.2 ± 0.2 Pa, respectively (see Supporting information). Thus, increasing shear rate during the formation of waxy or gel-like solids leads to a weaker fluid. One explanation is that energy added to the wax by imposing shear rate, breaks the bonds between wax particles

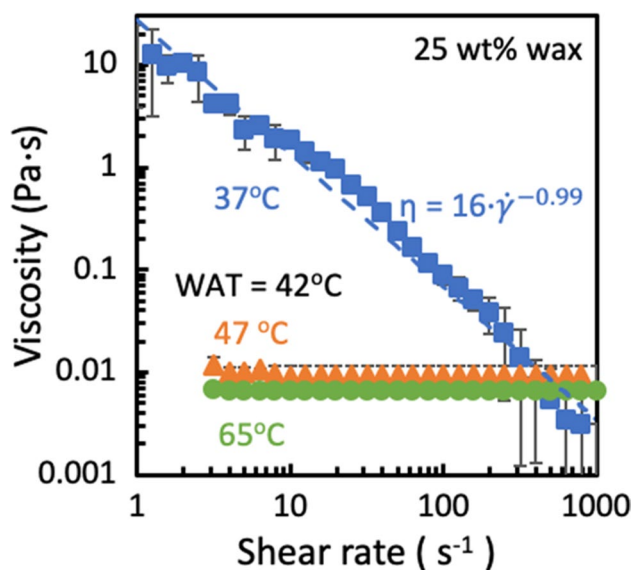


Fig. 2 Viscosity as a function of shear rate for 25 wt% wax at three different temperatures (65, 47, and 37 °C)

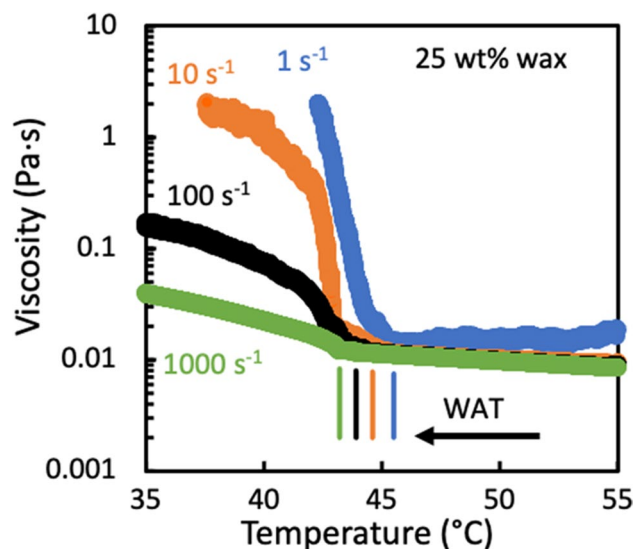


Fig. 3 Temperature ramp under induced flow for 25% wax/LMO sample for various shear rates. Colored vertical lines indicate WAT for each shear rate

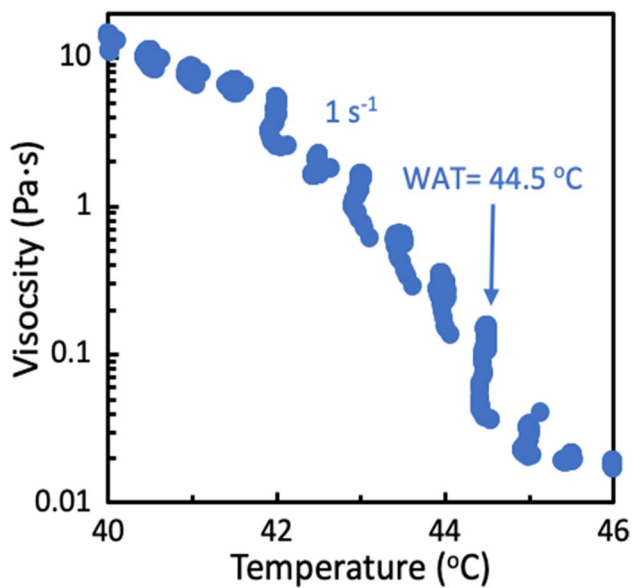


Fig. 4 Transient viscosity using isothermal steps to measure WAT under shear for 25% wax/LMO sample at 1 s^{-1}

and degrades the larger length scale or gel-like structure (E1-Gamal 1998). Hydrate slurries also present a similar trend in which viscosity decreases upon increasing shear rate (Thota 2016; Webb et al. 2013).

Since temperature ramps include some uncertainty defining a WAT, experiments using isothermal steps alternatively measured WAT (Fig. 4). At the same shear rates as the temperature ramps (1, 10, 100, and 1000 s^{-1}), the WAT was found to be 44.5, 44.0, 43.0, and $43.0 \text{ }^\circ\text{C}$. The standard deviation for isothermal step experiments was less than $0.5 \text{ }^\circ\text{C}$. A ratio of viscosity ~ 5 was used to identify WAT for both temperature ramps and isothermal step rheology experiments. Overall, WAT for 25 wt% wax in LMO measured with isothermal steps was similar to those measured with temperature ramp, but slightly lower ($0.2\text{--}1 \text{ }^\circ\text{C}$). This slight difference indicates that determining WAT is not only affected by shear rate but also temperature gradient. Since the temperature variability was eliminated in peak hold measurements, we can better see the effect of shear rate on WAT independent of temperature gradient. Overall, the WATs from both methodologies are in agreement ($\leq 1 \text{ }^\circ\text{C}$) across the full range of shear rates. Since temperature ramp experiments are faster than isothermal steps, WAT measurements from temperature ramps will be presented across different concentrations.

Cooling rate effects on WAT for 25 wt% wax

Cooling rate can also change the WAT (Chala et al. 2018; Ruwoldt et al. 2018). Decreasing the temperature gradient at constant shear rate depresses wax appearance temperatures.

For 25 wt% wax at 100 s^{-1} , WAT decreased from 43.9 to $40.1 \text{ }^\circ\text{C}$ when changing the cooling rate from 0.2 to $10 \text{ }^\circ\text{C}/\text{min}$. Similarly, WAT changed from 45.5 to $41.1 \text{ }^\circ\text{C}$ at 1 s^{-1} (Fig. 5). These findings are similar to samples of anhydrous milk fat and lard where solid content increases up to 10% upon decreasing the cooling rate from 5 to $0.1 \text{ }^\circ\text{C}/\text{min}$. Solid fat aggregates can trap liquid similar to wax droplets resulting in higher viscosity (Campos et al. 2002).

At slower cooling rates, small wax particles can aggregate and form larger clusters more readily. Waxy oil with larger wax particles has higher viscosity than waxy oil with smaller particles, so higher WATs have been measured for slower cooling rates (Chang et al. 2000). Faster cooling rates also resulted in lower gelation temperatures in asphaltene mixtures with crude oil (Venkatesan 2003), so our findings are consistent with the literature.

Increasing cooling rate raised yield stress for 25 wt% wax (see Supporting information). Cooling rate effect on yield stress is not monotonic and is dependent on the wax/gel failure mechanism. Yield stress increases with increasing cooling rate in case of adhesive failure while decreasing in case of cohesive failure (Lee et al. 2008). In our experiments, cooling rates appear to be below the delineation point, so the waxy gel breaks adhesively between the gel and metal surface. Higher cooling rates could not be attained using the vane and cup geometry. Delineation point for a waxy oil of 15 wt% gulf wax, 33 wt% kerosene, and wt% mineral oil has been measured using Couette geometry to be $7 \text{ }^\circ\text{C}/\text{h}$, which is larger than cooling rates obtained here (Lee et al. 2008).

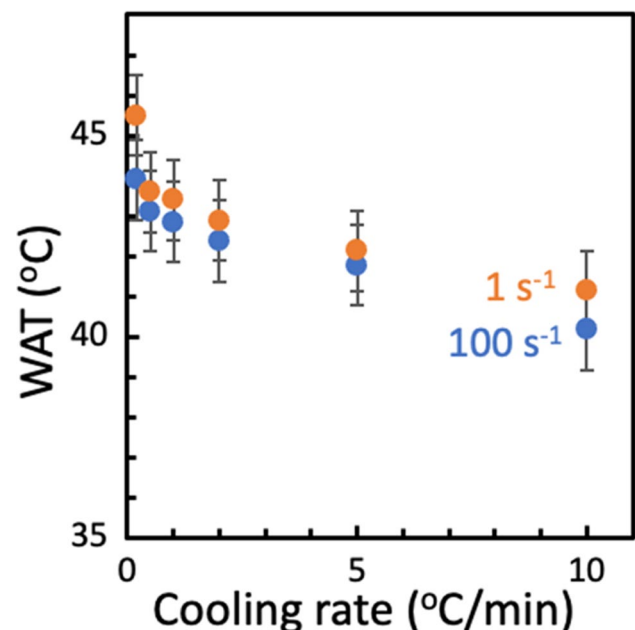


Fig. 5 WAT as a function of cooling rate from temperature ramp experiments under induced flow for 25% wax/LMO sample at shear rates 1 and 100 s^{-1}

Concentration effects on WAT under flow

Building upon WAT measurements for a 25 wt% paraffin wax in mineral oil, correlations between WAT and wax concentration were explored. Temperature ramp experiments for wax concentration from 5 to 50 wt% found that concentration more dramatically changes WAT than shear rate. On one hand, by increasing concentration from 5 to 50 wt%, WAT increased more than 20 °C (see Supporting information). On the other hand, decreasing shear rate from 1000 to 1 s⁻¹ at a constant temperature gradient increased WAT up to 2 °C. Thus, changing wax concentration from 10 to 15 wt% gave a 4 °C change in WAT that increasing shear rate from 1 to 1000 s⁻¹ did not achieve. Therefore, wax concentration is more important in determining WAT than shear rate in waxy mineral oil. Strong concentration-dependent rheological properties are common in particulate systems, which will be discussed more in this section.

Steady-state flow experiments were done for all wax concentrations at 5 °C below the WAT. Although all waxy oil mixtures showed shear thinning 5 °C below the WAT, the extent of shear thinning varied at different wax concentrations. At 5 and 10 wt% wax content, viscosity decreased by 2 orders of magnitude upon increasing shear rate from 1 to 1000 s⁻¹. However, for 15, 25, 35 wt% wax content, viscosity decreased by 5 orders of magnitude by increasing the shear rate from 1 to 1000 s⁻¹ (see Supporting information).

Analyzing the non-Newtonian behavior, shear thinning was modeled using a power law or Ostwald de Maele model following the expression: $\eta = k\dot{\gamma}^{n-1}$, where η = viscosity (Pa·s), k = consistency, $\dot{\gamma}$ = shear rate (s⁻¹), n = power law index. Both power law parameters varied with wax concentration (Table 1). R-squared values ranged from 0.96 to 0.99, so the model fits the rheological response well. On one hand, the consistency parameter k generally increased with wax concentration. Since the k parameter is indicative of viscosity, an increasing k with wax concentration was expected. On the other hand, the power law index (n) generally decreases with increasing wax content. Power law index is close to zero, which is commonly observed in shear banding systems, such as wormlike micelles (Hu and Lips 2005). Thus, discontinuities in velocity profiles analogous to shear bands

Table 1 Summary of power law index for shear thinning behavior of waxy oil samples at 5 °C below WAT

Wax content (wt%)	k	n
5	0.70	0.52
10	1.3	0.42
15	17	0.01
25	16	0.010
35	44	0.00
100	1700	0.00

may be relevant in waxy oils, which could serve as a topic for future work.

Viscosity at 5 °C above their WAT was almost constant with respect to shear rate and independent of wax concentration (Fig. 6). Conversely, at a constant shear rate, viscosity increased strongly with wax content after wax appearance, i.e., at 5 °C below the WAT. Viscosity increases with concentrations to the power of 1.5. Several equations have been proposed to correlate viscosity with concentration in suspensions, such as Einstein equation for dilute solutions of spherical particles (Stickel and Powell 2005). The increase in viscosity in our experiments was much larger than viscosities calculated by the Einstein equation; the wax concentrations were outside the dilute concentration regime and may not generate spherical wax particles. Also, the strongly shear-thinning nature of the waxy mixtures requires reporting viscosity at more than one shear rate to correlate with concentration. In another system at higher concentrations, the effect of solid concentration in biomass slurries showed increased with concentration to the power of 2.45, which is similar to our findings for waxes (Cruz 2013).

WAT under static conditions

Static conditions were studied using visual and thermal techniques. WAT at static condition will be compared with WAT under flow.

Visual observations of phase change behavior of waxy/light oil samples were determined using a temperature-controlled water bath. Lower wax concentrations showed a larger gap between cloud point and pour point temperatures

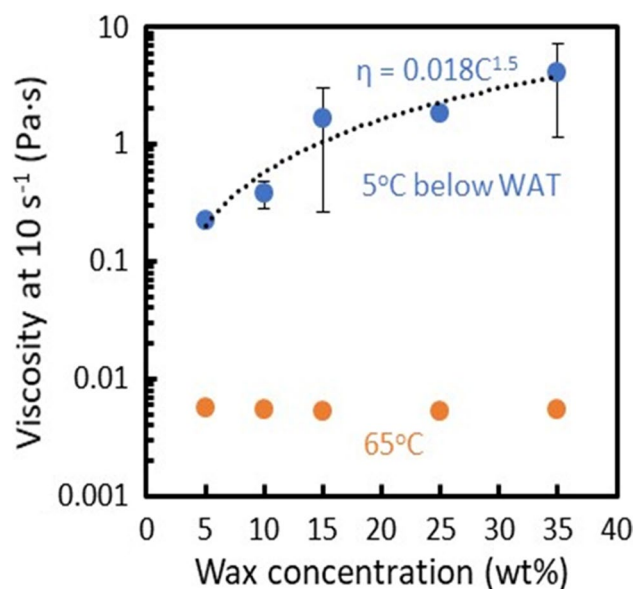


Fig. 6 Viscosity of LMO/wax samples at 5 °C below WAT and shear rate of 10 s⁻¹ with cooling rate of 0.2 °C/min

than higher concentrations. Differences between cloud point and pour point decreased with wax concentration. No cloud point was observed in the solution with 50% wax; rather, the sample suddenly underwent a phase change from liquid to solid at 50 °C (Fig. 7). Smaller gaps between cloud point and pour point temperatures may result from the mixtures reaching solid–liquid equilibrium very quickly (Dantas Neto et al. 2009).

Using DSC, thermal investigation of the WAT was achieved by identifying the onset temperature in the exothermic curve. Enthalpy increased as wax content increased. Wax appearance is an exothermic process and the amount of heat released as a result of wax appearance is dependent on carbon content and corresponds to wax concentration, which agrees with other studies (Alcazar-Vara and Buenrostro-Gonzalez 2011; Hansen et al. 1991).

Wax appearance temperatures measured using DSC were lower than water bath experiments by 4 to 5 °C. A higher cooling rate (10 °C/min) was used following ASTM D4419-90 (Chala et al. 2018), for DSC measurements, while water bath experiments employed a significantly lower cooling rate of 1 °C/h. Cooling rate affects wax crystallization and growth. At lower cooling rates, the growth stage of crystallization could be more important than nucleation and lead to higher WATs (Japper-Jaafar et al. 2016a).

WATs were determined for all wax concentrations using temperature ramps of 10 °C/min and a shear rate of 1000 s⁻¹. Results are in a good agreement (within 0.8 °C) with DSC, with cooling rate of 10 °C/min, which verifies that cooling

rate has a stronger effect on creating solid wax particles than shear rate (see Supporting information).

Conclusions

Wax appearance temperatures in a two-component system of mineral oil and paraffin wax were quantified as a function of shear rate, cooling rate, and wax concentration. Wax concentration had the largest impact on WAT. When increasing wax concentration from 5 to 50% wt, WAT increased by 20 °C. Strong dependency of solution's viscosity to concentration of solid particles scaled as a power law, similar to other systems. Additionally, shearing waxy oils from 1 to 1000 s⁻¹ decreases WAT about 2 °C. High shear rate does not allow particles to be in contact with each other for long periods of time and form bigger clusters. Increasing shear rate from 0 to 1000 s⁻¹ lowered yield stress from about 416 to 8 Pa. So, waxy solids formed at higher shear rates break easier, which could translate to easier pipeline flow restart. Also, increasing cooling rate from 0.2 to 10 °C/min, results up to 4.4 °C decrease in WAT and increasing yield stress. Decrease in WAT might be because of presence of large-sized wax particles, which more readily form at lower cooling rates; cooling rate can be different based on reservoir, environment temperature, and pipe diameter (Singh et al. 1999). Overall, these findings would recommend that maintaining higher shear rates in pipelines transporting waxy crude oil could improve flow assurance.

Supplementary Information The online version contains supplementary material available at <https://doi.org/10.1007/s00397-021-01284-2>.

Acknowledgements The authors acknowledge Uchenna Asogwa and Kayla Piezer for helping with some experiments. Acknowledgment is made to the Donors of the American Chemical Society Petroleum Research Fund (57692-ND9) for support of this research.

Author contribution The manuscript was written through contribution of all authors. All authors have given approval to the final version of the manuscript.

Funding American Chemical Society Petroleum Research Fund (57692-ND9)

References

- Alcazar-Vara LA, Buenrostro-Gonzalez E (2011) Characterization of the wax precipitation in Mexican crude oils. *Fuel Process Technol* 92:2366–2374. <https://doi.org/10.1016/j.fuproc.2011.08.012>
- Campos R, Narine SS, Marangoni AG (2002) Effect of cooling rate on the structure and mechanical properties of milk fat and lard. *Food Res Int* 35:971–981. [https://doi.org/10.1016/S0963-9969\(02\)00159-X](https://doi.org/10.1016/S0963-9969(02)00159-X)

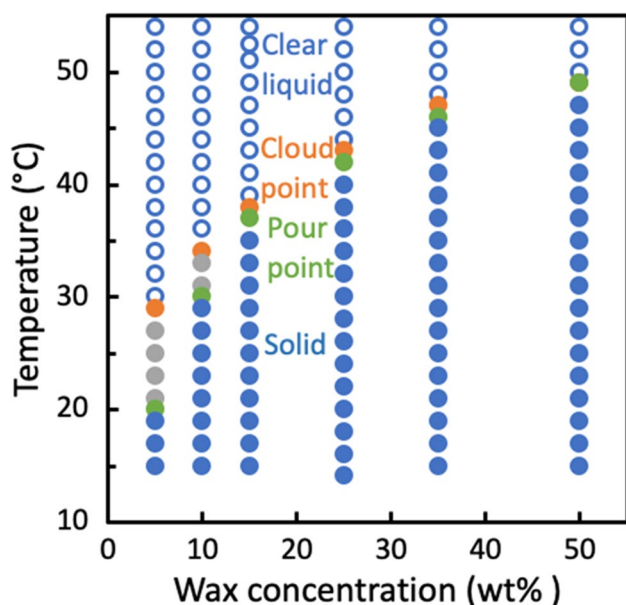


Fig. 7 Phase behavior of LMO/wax samples observed from 65 to 15 °C in water bath (between cloud point and pour point is cloudy liquid)

- Chala GT, Sulaiman SA, Japper-Jaafar A (2018) Flow start-up and transportation of waxy crude oil in pipelines—a review. *J Non-Newton Fluid Mech* 251:69–87. <https://doi.org/10.1016/j.jnnfm.2017.11.008>
- Chang C, Boger DV, Nguyen QD (2000) Influence of thermal history on the waxy structure of statically cooled waxy crude oil. *SPE J* 5:148–157. <https://doi.org/10.2118/57959-PA>
- Coutinho JAP, Daridon J-L (2005) The limitations of the cloud point measurement techniques and the influence of the oil composition on its detection. *Pet Sci Technol* 23:1113–1128. <https://doi.org/10.1081/LFT-200035541>
- Cruz AG (2013) Impact of high biomass loading on ionic liquid pretreatment Biotechnology for Biofuels 6 <https://doi.org/10.1186/1754-6834-6-52>
- Dantas Neto A, Gomes E, Barros Neto E, Dantas T, Moura C (2009) Determination of wax appearance temperature (WAT) in paraffin/solvent systems by photoelectric signal and viscosimetry Brazilian Journal of Petroleum and Gas 3:149–157
- Dimitriou CJ, McKinley GH (2014) A comprehensive constitutive law for waxy crude oil: a thixotropic yield stress fluid. *Soft Matter* 10:6619–6644. <https://doi.org/10.1039/C4SM00578C>
- Dimitriou CJ, McKinley GH, Venkatesan R (2011) Rheo-PIV analysis of the yielding and flow of model waxy crude oils. *Energy Fuels* 25:3040–3052. <https://doi.org/10.1021/ef2002348>
- E1-Gamal IM (1998) Combined effects of shear and flow improvers: the optimum solution for handling waxy crudes below pour point *Colloid Surf* 135:283–291 [https://doi.org/10.1016/S0927-7757\(97\)00261-6](https://doi.org/10.1016/S0927-7757(97)00261-6)
- Flavio S. Ribeiro, Paulo R. Souza Mendes, Sergio L. Braga (1997) Obstruction of pipelines due to paraffin deposition during the flow of crude oils *Int J Heat Mass Transfer* 4:4319–4328
- Freund M, Csikós R, Keszthelyi S, Mózes GY (1982) Paraffin products: properties, technologies, applications. Elsevier, Amsterdam
- García MdC (2000) Crude oil wax crystallization. The effect of heavy n-paraffins and flocculated asphaltene energy and fuels 14:1043–1048. <https://doi.org/10.1021/ef0000330>
- Hagen RDRLPN (1993) Viscoelastic characterization of medium consistency pulp suspensions *Can J Chem Eng* 71 <https://doi.org/10.1002/cjce.5450710504>
- Hamada H et al (2010) Effects of polyglycerol esters of fatty acids and ethylene-vinyl acetate co-polymer on crystallization behavior of biodiesel. *Eur J Lipid Sci Technol* 112:1323–1330. <https://doi.org/10.1002/ejlt.201000359>
- Hammami A, Ratulowski J, Coutinho JA (2003) Cloud points: can we measure or model them? *Pet Sci Technol* 21:345–358. <https://doi.org/10.1081/LFT-120018524>
- Hansen AB, Larsen E, Pedersen WB, Nielsen AB (1991) Wax precipitation from North Sea crude oils Precipitation and dissolution of wax studied by differential scanning calorimetry. *Energy Fuels* 5:914–923
- Hénaut I, Vincké O, Brucy F (1999) Waxy crude oil restart: mechanical properties of gelled oils SPE Annual Technical Conference and Exhibition <https://doi.org/10.2118/56771-MS>
- Hsu J, Brubaker J Wax deposition measurement and scale-up modeling for waxy live crudes under turbulent flow conditions. In: International Meeting on Petroleum Engineering, 1995. Society of Petroleum Engineers, pp 241–250. <https://doi.org/10.2118/29976-MS>
- Hu YT, Lips A (2005) Kinetics and mechanism of shear banding in an entangled micellar solution. *J Rheol* 49:1001–1027. <https://doi.org/10.1122/1.2008295>
- Japper-Jaafar A, Bhaskoro P, Mior Z (2016a) A new perspective on the measurements of wax appearance temperature: comparison between DSC, thermomicroscopy and rheometry and the cooling rate effects *J Pet Sci Eng* 147:672–681 <https://doi.org/10.1016/j.petrol.2016.09.041>
- Japper-Jaafar A, Bhaskoro PT, Mior ZS (2016b) A new perspective on the measurements of wax appearance temperature: comparison between DSC, thermomicroscopy and rheometry and the cooling rate effects *J Pet Sci Eng* 147:672–681 <https://doi.org/10.1016/j.petrol.2016.09.041>
- Kane M, Djabourov M, Volle J-L, Lechaire J-P, Frebourgc G (2002) Morphology of paraffin crystals in waxy crude oils cooled in quiescent conditions and under flow. *Fuel* 82(2003):127–135
- Kurniawan M, Subramanian S, Norrman J, Paso K (2018) Influence of microcrystalline wax on the properties of model wax-oil gels. *Energy Fuels* 32:5857–5867. <https://doi.org/10.1021/acs.energyfuels.8b00774>
- Lashkarbolooki M, Esmaeilzadeh F, Mowla D (2011) Mitigation of wax deposition by wax-crystal modifier for Kermanshah crude oil *J Dispers Sci Technol* 32:975–985 <https://doi.org/10.1080/01932691.2010.488514>
- Lee HS (2008) Computational and rheological study of wax deposition and gelation in subsea pipelines. The University of Michigan
- Lee HS, Singh P, Thomason WH, Fogler HS (2008) Waxy oil gel breaking mechanisms: adhesive versus cohesive failure. *Energy Fuel* 22:480–487. <https://doi.org/10.1021/ef700212v>
- Li H, Zhang J, Song C, Sun G (2015) The influence of the heating temperature on the yield stress and pour point of waxy crude oils. *J Petrol Sci Eng* 135:476–483. <https://doi.org/10.1016/j.petrol.2015.10.010>
- Lin M, Li C, Yang F, Ma Y (2011) Isothermal structure development of Qinghai waxy crude oil after static and dynamic cooling. *J Petrol Sci Eng* 77:351–358. <https://doi.org/10.1016/j.petrol.2011.04.010>
- Macosko CW (1994) Rheology: principles, measurements, and applications. Wiley-VCH, New York
- Mezger T (2011) The Rheology Handbook, 4th edn. Vincentz Network, Hanover
- Rønningsen H (1992) Rheological behaviour of gelled, waxy North Sea crude oils *J Pet Sci Eng* 177–213
- Ruwoldt J, Kurniawan M, Oschmann H-J (2018) Non-linear dependency of wax appearance temperature on cooling rate. *J Petrol Sci Eng* 165:114–126. <https://doi.org/10.1016/j.petrol.2018.02.011>
- Singh P, Fogler HS, Nagarajan N (1999) Prediction of the wax content of the incipient wax-oil gel in a pipeline: An application of the controlled-stress rheometer. *J Rheol* 43:1437–1459. <https://doi.org/10.1122/1.551054>
- Singh P, Venkatesan R, Fogler HS, Nagarajan N (2000) Formation and aging of incipient thin film wax-oil gels. *AIChE J* 46:1059–1074. <https://doi.org/10.1002/aic.690460517>
- Stickel JJ et al (2009) Rheology measurements of a biomass slurry: an inter-laboratory study. *Rheol Acta* 48:1005–1015. <https://doi.org/10.1007/s00397-009-0382-8>
- Stickel JJ, Powell RL (2005) Fluid mechanics and rheology of dense suspensions. *Annu Rev Fluid Mech* 37:129–149. <https://doi.org/10.1146/annurev.fluid.36.050802.122132>
- Sun G, Zhang H, Liu D, You J, Yang F, Li C, Yao B (2019) Impact of the composition and content of dissolved-state paraffins in model oil on the aggregation state of asphaltene and the soft water-in-model oil emulsion. *Energy Fuels* 33:12191–12201. <https://doi.org/10.1021/acs.energyfuels.9b02781>
- Tarantino G et al (2016) Characterization and evaluation of waxy crude oil flow. *Braz J Chem Eng* 33:1063–1071. <https://doi.org/10.1590/0104-6632.20160334s20150103>
- Theyab MA (2018) Fluid flow assurance issues: literature review *SciFed Journal of Petroleum* 2:1–11
- Theyab MA, Yahya SY (2018) Introduction to wax deposition *Int J Pet Res* 2:126–131 <https://doi.org/10.18689/ijpr-1000122>
- Thota ST (2016) Mitigation of Wax in Oil Pipelines *Int J Eng Res Rev* 4:39–47

- Thota ST, Onyeanuna CC (2016) Mitigation of wax in oil pipelines Int J Eng Res Rev 4:39–47
- Vargas GG, Soares EJ, Thompson RL, Sandoval GAB, Andrade RM, Campos FB, Teixeira A (2018) Emulsion effects on the yield stress of gelled waxy crude oils. Fuel 222:444–456. <https://doi.org/10.1016/j.fuel.2018.01.105>
- Venkatesan R (2003) The effect of asphaltenes on the gelation of waxy oils Energy & Fuels:1630–1640 <https://doi.org/10.1021/ef034013k>
- Visintin RFG (2005) Rheological behavior and structural interpretation of waxy crude oil Gels. Langmuir 21:6240–6249. <https://doi.org/10.1021/la050705k>
- Wagner NJ, Brady JF (2009) Shear Thickening in Colloidal Dispersions Physics Today 62:27–32. <https://doi.org/10.1063/1.3248476>
- Webb EB, Koh CA, Liberatore MW (2013) Rheological properties of methane hydrate slurries formed from AOT + water + oil microemulsions Langmuir 29:10997–11004 <https://doi.org/10.1021/la4022432>
- Wessel R, Ball RC (1992) Fractal aggregates and gels in shear flow. Phys Rev A 46:R3008–R3011. <https://doi.org/10.1103/PhysRevA.46.R3008>
- Winterton RHS (1970) Van Der Waals Forces Contemporary Physics 11:559–574. <https://doi.org/10.1080/00107517008202194>
- Yang F, Zhao Y, Sjöblom J, Li C, Paso KG (2015) Polymeric wax inhibitors and pour point depressants for waxy crude oils: a critical review J Dispers Sci Technol 36:213–225 <https://doi.org/10.1080/01932691.2014.901917>
- Zhao Y, Paso K, Norrman J, Ali H, Sørland G, Sjöblom J (2015) Utilization of DSC, NIR, and NMR for wax appearance temperature and chemical additive performance characterization. J Therm Anal Calorim 120:1427–1433. <https://doi.org/10.1007/s10973-015-4451-1>
- Zhu T, Walker JA, Liang J (2008) Evaluation of wax deposition and its control during production of Alaska north slope oils. University of Alaska. <https://doi.org/10.2172/963363>

Publisher's note Springer Nature remains neutral with regard to jurisdictional claims in published maps and institutional affiliations.